A fully integrated chip-scale optomechanical oscillator

Xingsheng Luan,[1,*] Yongjun Huang,[1,2,*] Ying Li,[1] James F. McMillan,[1] Di Wang,[1] Archita Hati,[3] David A. Howe,[3] Mingbin Yu[4], Guoqiang Lo[4], Dim-Lee Kwong[4], and Chee Wei Wong,[1,*]

[1]*Optical Nanostructures Laboratory, Columbia University, New York, NY 10027, USA*
[2]*Key Laboratory of Broadband Optical Fiber Transmission & Communication Networks, School of Communication and Information Engineering University of Electronic Science and Technology of China, Chengdu, 611731, China*
[3]*National Institute of Standards and Technology, Boulder, CO 80303, USA*
[4]*The Institute of Microelectronics, 11 Science Park Road, Singapore 117685, Singapore*
**Author e-mail address: xl2354@columbia.edu, yh2663@columbia.edu; cww2104@columbia.edu*

Abstract: We demonstrate a chip-scale slot-type photonic crystal optomechanical oscillator fully integrated with an on-chip waveguide Ge photoreceiver, which exhibits high-harmonic tunable RF oscillations and high-quality optical resonances with controlled detuned continuous-wave laser drive.

OCIS codes: (230.5750) Optical resonators, (220.4880) Optomechanics, (230.4910) Oscillators

1. Introduction

In the past several years, much attention has focused on the mesoscopic cavity optomechanics [1] due to the breakthroughs of nano fabrications and advanced measurement technologies. In the nano-scale cavity, the optical and mechanical energies can couple well, resulting in some novel properties e.g. dynamical back-action and parameters instability, and has found applications such as quantum cooling, precision measurements, and photon clock [1]. When the mechanical modes are optically amplified by laser drive, the optomechanical cavity becomes an oscillator with sustained mechanical oscillations [2]. Several optomechanical oscillator (OMO) realizations including silicon nitride microring, silica microtoroid, and photon crystal (PhC) cavity are reported in recent years [2–4]. However, most of the OMO inclusions need an external photon-electronic detector to capture modulated optical signal and then obtain the mechanical oscillations, which would restrict the practical on-chip applications. Here we demonstrate a chip-scale slot-type PhC OMO fully integrated with an on-chip waveguide Ge photoreceiver for the first time to our knowledge, which exhibits high-harmonic tunable RF oscillations and high-quality optical resonances with controlled detuned continuous-wave laser drive.

2. Chip design and characteristics

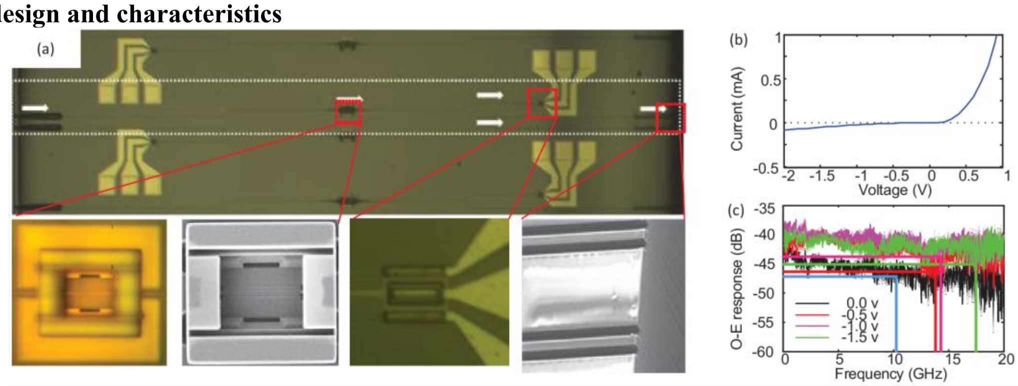

Fig. 1. (Color online) (a) Designed fully-integrated OMO chipset. Zoom-in plots are (from left to right) optical and SEM images of the OMO, optical image of the on-chip waveguide Ge photoreceiver, and SEM image of the silicon coupling waveguide. (b) I-V curve for the Ge photoreceiver. (c) Optical-electronic response bandwidth of the Ge photoreceiver under different inverse bias voltages.

The proposed fully-integrated OMO chipset is shown in Fig. 1(a). A slot-type PhC optomechanical cavity [4] is placed in the center region. The input laser is coupled into the silicon waveguide by lens and then reach to the slot-type PhC cavity. After the PhC cavity, the laser light modulated by dynamical back-action splits to two ways for comparisons, one transmitted to the on-chip Ge photoreceiver and another one went to the other side of the chip and then coupled out by another lens. The silicon waveguides at two sides of the chip and near the PhC cavity are tapered for impedance matching and decreasing the reflection losses. The I-V curve for the Ge photoreceiver is firstly demonstrated and the result is shown in Fig. 2(b), which indicates a typical diode characteristic. On another hand, to obtain a wide response bandwidth and maintain a good optical-electronic conversion rate, the length of the Ge photoreceiver should be chosen properly. Here we choose the length as 25 μm and obtain the optical-electronic response bandwidth as shown in Fig. 1(c). It can be seen that, with different inverse bias voltages, we can obtain at least 10 GHz response bandwidth, which ensure to cover the harmonic mechanical oscillations up to 17 GHz.

3. Results

We build the setup as shown in Fig. 2(a) to demonstrate the optical resonances and mechanical oscillations. A high performance tunable scanning laser generates stabilize lights (1510-1630 nm), then passes through optical amplification by EDFA and large reflection power protection by isolator, reaches to polarization controller and polarizer to outcome a TE polarization light for best coupling into the Silicon waveguide and PhC cavity. After optical and mechanical interaction in the cavity, the off-chip slow and fast detectors and on-chip Ge photoreceiver are used to detect optical and mechanical signals. Firstly, from the measured optical transmissions as shown in Fig. 2(b) two modes are obtained, and from FEM simulations (see inset plots in Fig. 2(b)) by Comsol 4.3b the second mode (1541.5 nm) is corresponding to fundamental optical mode. Zoom-in plot shows a typical Lorentz feature and the fitted optical loaded quality factor value is Q= 6.61×10^4. We further demonstrate the thermal nonlinear effects of the optical resonance under increasing input laser powers, as shown in Fig. 2(c). Then, by pumping a fix input laser at blue-detuning wavelength with low input power of 0 dBm, both off-chip and on-chip detectors capture the mechanical resonance near 110.3 MHz, as shown in Fig. 2(d) and (e). The mechanical quality factor measured by two different detectors match pretty well. The noise floor for Ge-detector is ~-100 dBm, which is much lower than the New Focus detector we use. From FEM simulation for the mechanical resonance of the OMO cavity, as shown in Fig. 2(f), the fundamental modes operates at 148 MHz, which shows slight frequency different due to the fabrication tolerance. Finally, to obtain the optical driving OMO oscillations, we pump a higher input laser power up to 23 dBm by EDFA and capture a very plentiful mechanical oscillations up to 7 GHz (by off-chip detector), as shown in Fig. 2(g). More harmonics will be obtained by higher performance instruments. It indicates that the designed OMO has applications for RF clock and we will further demonstrate the stability of each frequency tone in future.

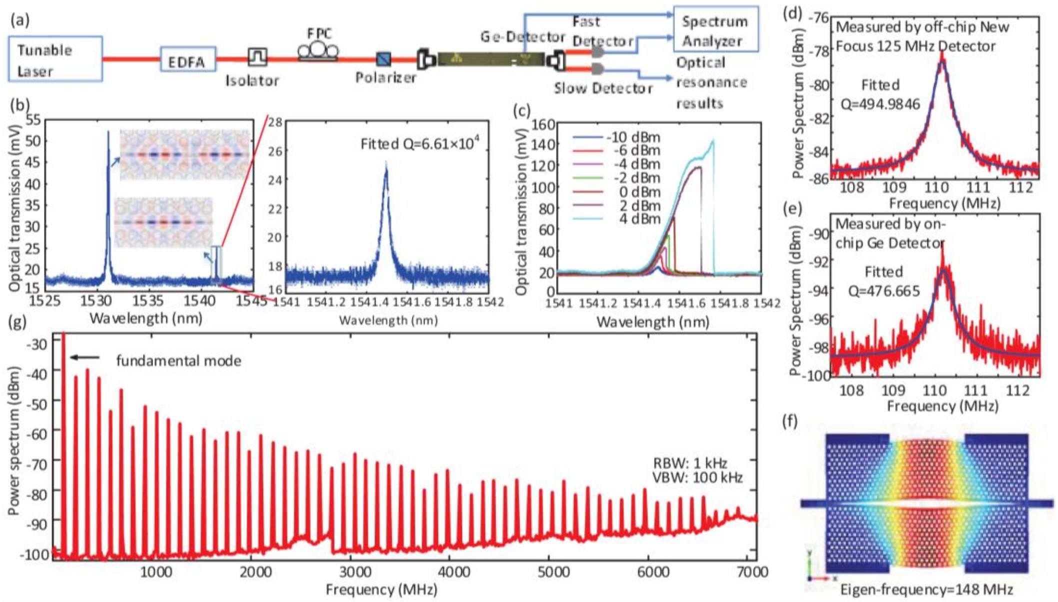

Fig. 2. (Color online) (a) Schematic diagram of the experimental setup for measurements of optical resonances and mechanical oscillations. Tunable laser used here is Santec TSL 510-C (1510-1630 nm). EDFA indicates the laser power amplifier. FPC is polarization controller. Isolator is used to protect the EDFA when large reflection power occurred. Polarizer is used to filter the wanted TE polarization input to the Silicon waveguide and PhC cavity. The on-chip Ge photoreceiver and off-chip fast detector (New Focus 125 MHz) are used to detect the output light modulated by dynamical back-action and then analyzed by the RF Power Spectrum Analyzer. Slow detector is used to monitor the optical transmission. (b) Optical transmission result which shows two resonance modes. The inset plots indicate the simulated electrical field distributions at such two optical resonances. The zoom in plot shows a very high optical loaded quality factor up to 6.61×10^4. (c) Optical transmissions under different input powers. (d) RF power spectrum detected by off-chip detector. (e) RF power spectrum detected by on-chip Ge photoreceiver. (f) FEM simulated mechanical displacement at Eigen-frequency 148 MHz. (g) Harmonics of the OMO oscillations under an input laser power of 23 dBm.

4. References

[1] M. Aspelmeyer, T.J. Kippenberg, F. Marquardt, "Cavity Optomechanics," arXiv:1303:0733 (2013).
[2] S. Tallur, S. Sridaran, and S. A. Bhave, "A monolithic radiation-pressure driven, low phase noise silicon nitride opto-mechanical oscillator, Opt. Express, 19, 24522-24529 (2011).
[3] M. Hossein-Zadeh, and K. J. Vahala, "An optomechanical oscillator on a silicon chip," IEEE J. Selected Topics in Quantum Electronics, 16, 276-287 (2010).
[4] J. Zheng, Y. Li, M. S. Aras, A. Stein, K. L. Shepard, and C. W. Wong, "Parametric optomechanical oscillation in two-dimensional slot-type high-Q photonic crystal cavities," Appl. Phys. Lett., 100, 211908 (2012).